ACS OMEGA

Open Access

http://pubs.acs.org/journal/acsodf

Article

Role of GO and Photoinitiator Concentration on Curing Behavior of PEG-Based Polymer for DLP 3D Printing

Men Thi Hong Nguyen, Jong Hoon Kim, Woo Tae Jang, Yun Jae Jung, Eun Jin Park, Tai Hwan Ha, Sang Jung Ahn,* and Young Heon Kim*

Cite This: *ACS Omega* 2024, 9, 3287−3294

Read Online

ACCESS | Metrics & More | Article Recommendations

ABSTRACT: Photocuring kinetics in photopolymerization-based three-dimensional (3D) printing processes have gained significant attention because they determine the final dimension accuracy of the printed structures. In this study, the curing kinetics of liquid-light-curable resins, including water-dispersed graphene oxide (GO) and ultraviolet (UV)-cured acrylic resins, were investigated during digital light processing (DLP) 3D printing. Various stable composites of water-dispersed GO and UV-cured acrylic resin were prepared to fabricate 3D structures for cure-depth measurements. Several factors, including the UV-exposure conditions, photoinitiator concentration, and composition of the photopolymer resin, were found to significantly affect the cure-depth characteristics of the printed structures. The photocuring depth of the polymeric resin system was investigated as a function of the photoinitiator concentration. In addition, the study showed that the introduction of GO played a significant role in controlling the performance of the highly cross-linked network and the thickness of the cured layer. The curing characteristics of functional photocurable polymer-based DLP 3D printing contribute to process development and improvement of the quality of printed microstructures for industrial applications.

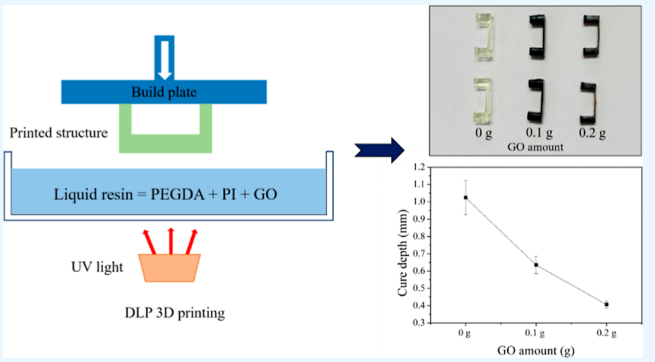

1. INTRODUCTION

Photopolymerization, which uses photons to initiate photochemical reactions in organic materials and transform them into polymeric materials, is a well-accepted technology for manufacturing polymers. Significant advantages can be realized from using photopolymerization over thermally initiated polymerization, including a high curing rate and low energy consumption.[1,2] Moreover, the utilization of light to initiate polymerization enables easy spatial and temporal control of the chemical reactions.[3] Fabricating parts and products using three-dimensional (3D) printing techniques based on photopolymerization has gained considerable attention because of its ability to fabricate complex 3D structures and controlled internal structures.[4] 3D printing consists of several fabrication methods such as stereolithography, fused deposition modeling, and selective laser sintering.[5−7] Stereolithography is widely used for the manufacture of 3D polymer parts and involves the polymerization of a reactive system. Digital light processing (DLP), a highly advanced 3D printing technique, has been used to fabricate polymeric parts with high resolution, high print speed, and smooth surface finish.[8,9] Furthermore, this method is based on a layer-by-layer polymerization of the entire photopolymer surface by using a projector source light. DLP 3D printing has been adapted for the 3D processing of highly cross-linked materials with mechanical and electrical properties.[10,11] Using the DLP method, custom dental models, direct generation of molds, medical devices, and automotive parts can be fabricated.[12−14]

Photocuring-based DLP methods are considered to be the most promising 3D printing techniques, because they can significantly enhance printing precision. In particular, the study of the reaction mechanism and curing kinetics of photopolymers is vital in the quality improvement of parts manufactured via 3D printing.[7,15−17] The typical curing behavior of photopolymer resins is characterized by two parameters: the critical energy and penetration depth of the material. These parameters are used to determine the exposure energy required to achieve chemical cross-linking of the photocurable resins. Consequently, several strategies have been developed to control the cure depth using photocurable resins for accurate fabrication. Several parameters, such as light

Received: July 24, 2023
Revised: November 24, 2023
Accepted: December 25, 2023
Published: January 8, 2024

intensity, photoinitiator (PI) concentration, and composition of the photopolymer resin, are considered to affect monomer-to-final-polymer conversions.[18−20]

High-performance photopolymer resins for 3D printing via photopolymerization are based on monomers/oligomers, PIs, diluents, and different additives for the stabilization of the formulation.[21] Graphene oxide (GO)-based polymer composites have reinforced mechanical strength and improved electrical conductivity and gas barrier properties compared with neat polymers.[22,23] GO can be easily dispersed in the polymer matrix owing to the presence of functional groups, such as hydroxyls, epoxides, and carboxyls.[24,25] Furthermore, GO is compatible with organic polymers; hence, it has attracted considerable interest as a nanofiller for polymer nanocomposites. Polyethylene glycol diacrylate (PEGDA) is a nonbiodegradable polymer that has been widely utilized because of its nontoxicity, good hydrophilicity, and biocompatibility.

The degree of curing is a function of different parameters related to the resin composition and printer parameters. The effects of these parameters on the cure depth, fabricated using a photopolymer of PEGDA and a composite containing PEGDA and GO, have not been fully examined. In this study, we investigate the cure-depth behaviors of different photopolymer resins. GO-based polymer 3D structures are fabricated using DLP. The 3D structures were fabricated from a mixture of GO dispersed in a polymer matrix. The presence of GO can significantly affect the curing depth characteristics of 3D printed structures and control the light penetration inside the photosensitive resin. In addition, the exposure conditions of the DLP printer were adjusted to examine their influence on the cure-depth behavior. In photopolymerization for 3D printing, ultraviolet (UV)-sensitive PI is an essential component of the degree of curing. Therefore, the PI concentration in the acrylic polymer resin was also investigated to control the cure-depth behavior and achieve the optimal dimensional accuracy of the printed structures.

2. MATERIALS AND METHODS

2.1. Ink Preparation. PEGDA (M_n = 700) was used as the photocurable acrylate resin because of its nontoxicity and water-soluble polymeric characteristics. Photocurable resins generally consist of monomers or oligomers as the main component and a PI for the cross-linking reaction. To increase light absorption by the resin, PEGDA was mixed with PI Irgacure 819 via sonication. PEGDA was mixed with various PI concentrations within the range of 0.3−3 wt % to investigate the influence of PI concentration on the cure depth of printed structures.

GO can be dispersed directly in water or organic solvents.[26] The GO/water dispersion was formulated by dispersing GO in deionized water (DI) according to different GO powder quantities ranging from 0.01 to 0.2 g and 25 mL of DI. The solution was sonicated for 1 h to obtain a stable homogeneous GO/water dispersion. In this formulation, the introduction of GO into the dispersion in higher amounts led to a higher viscosity. It has been suggested that the viscosity of the mixture should not exceed 3 Pa·s to achieve good layer recovery.[27,28] Direct addition of GO powder to acrylic resins causes aggregation.[29,30] Consequently, GO/water dispersions were introduced into the acrylic resin.

The GO−polymeric composite was prepared by mixing different concentrated GO/water dispersions with 50 g of PEGDA. To enhance the UV-light absorption of the composites during 3D printing, a PI Irgacure 819 (1 wt %) was added with a fixed concentration of 1 wt %. The GO−polymeric mixture was sonicated to obtain formulations in which the polymeric medium remained stable. Liquid polymer inks must exhibit good printability, adhesion to substrates, and high resolution.

2.2. 3D Printing. All samples were 3D-printed using a DLP printer (Anycubic Photon S DLP 3D printer) at a wavelength of light source of 405 nm. The DLP printer used is a bottom-up printer with LCD shadow masking printing technology and a layer thickness resolution of 25−100 μm. Fabrication was performed using a light intensity of 3 mW/cm^2.

To investigate the cure-depth behavior of different photo-cross-linkable resins, the structures were designed with a dimension of thickness of 200 μm. The exposure times for a single layer were set to 5, 10, 20, 30, and 60 s. For the first layer, the exposure time was set to 60 s to enhance the adhesion of the printed structures to the bottom of the mount. Subsequently, the structures were removed from the mount and exposed to UV light for 30 min to completely cure the remaining liquid resin completely. The prepared samples were then ready for curing depth measurements. A digital caliper was used to measure the curing depths of the printed structures. For each investigation, we measured ten samples of printed structures. The caliper used for this study exhibited a resolution of 0.01 mm, resulting in a possible error of approximately ±10%.

2.3. Photopolymer Curing Kinetics. Photocurable resins are primarily classified into the following two types based on their polymerization mechanism: free-radical photopolymerization and cationic photopolymerization.[1] From an industrial perspective, free-radical photopolymerization is the most widely utilized method.[31,32] Free-radical photopolymerization occurs when radicals generated by PI are present in sufficient quantities to initiate the polymerization of the monomers. The photomerization kinetics in the fabrication of structures using stereolithography is governed mainly by the penetration depth of the curing light and the energy required for polymerization. When 3D microstructures are created using photocurable resins, vertical resolution along the light propagation direction is crucial for achieving dimensional accuracy of the structure. The key parameter in terms of the reactivity of the UV-curable suspension is the cure depth. The theoretical expression for the polymerization depth is derived from the Beer−Lambert law as follows[33]

$$C_d = D_p \ln\left(\frac{E}{E_c}\right) \quad (1)$$

where C_d is the thickness/depth of the cured resin. D_p is the penetration depth of the resin at which the penetrating light intensity reaches $1/e$ (approximately 37%) of the surface intensity. E is the exposure energy density on the resin surface, and E_c is the critical exposure energy or minimal exposure required to initiate polymerization. When the applied energy dose (E) exceeds the critical energy required, a solidified layer forms on the liquid resin surface. Based on eq 1, a semilog plot of C_d against E produces a linear graph referred to as the working curve specific to a given resin. The x-axis intercept of the working curve represents the critical energy (E_c), while the slope of the curve corresponds to the penetration depth (D_p) at the laser wavelength. E_c and D_p are both characteristic

https://doi.org/10.1021/acsomega.3c05378
ACS Omega 2024, 9, 3287−3294

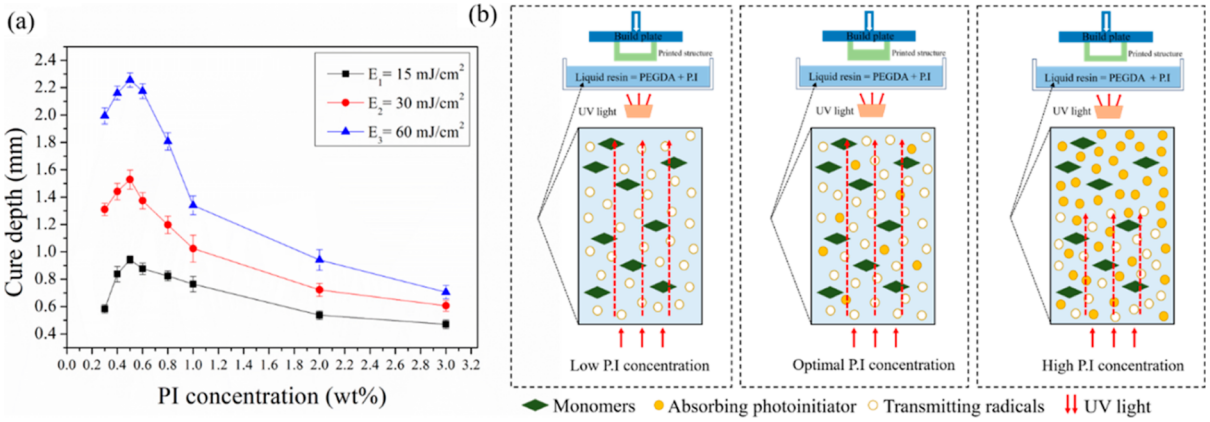

Figure 1. (a) Effect of different PI concentrations on the cure depth of the printed structures with different exposure energies. (b) Schematic representation of photopolymerization with different PI concentrations.

constants of the resin. The penetration depth indicates the material's sensitivity to variations in light output; a material with a lower D_p exhibits better performance when exposed to changes in exposure time or light source power, compared to a higher D_p.

Cure-depth tests and the obtained working curves are essential for characterizing photopolymers. The cure depth was determined by illuminating the photopolymer for different exposure times and measuring the thickness of the cross-linked networks. For a given resin, the polymerization depth depends on the light energy to which the resin is exposed. This energy can be controlled by adjusting the power of the light source and the exposure time (for projection systems) or the scanning speed (for laser systems). The exposure parameters can be selected to optimize the printing process and obtain the desired part properties. A comparison of the cure depths of different photopolymers is required to determine the optimal curing conditions for the best resolution of printed structures.

The absorbance and attenuation of incident light by the photopolymer material are essential for free-radical polymerization. The penetration depth is specific to each liquid resin and is related to its absorption characteristics and composition. The depth of light polymerization may differ for each photopolymer because of the PI composition differences, viscosity, composition of the resin, and power of the light source of the 3D printer selected.[16,32]

3. RESULTS AND DISCUSSION

3.1. Cure Depth vs PI Concentration—Critical PI Concentration. The key component in photopolymerization formulations is the PI, which acts as a bridge between the UV light source and the liquid resin mixture. The peak light-absorbing wavelength of the PI often matches the peak wavelength of the UV light source to maximize the photoinitiation rates.

Figure 1a shows the relationship between the cure depths as a function of PI concentration at different exposure energy doses. The examined polymeric resins were prepared by mixing PEGDA with different PI concentrations varying with 0.3, 0.4, 0.5, 0.6, 0.8, 1, 2, and 3 wt %. The polymeric resin consisting of 0.1 and 0.2 wt % PI concentration could not be printed successfully because of the insufficient light absorption of the liquid resin. In addition, the 4 wt % PI concentration caused saturation of the formulation, and the PI could not completely dissolve in the suspension. The exposure time was adjusted to 5, 10, and 20 s, corresponding to exposure energy doses of 15, 30, and 60 mJ/cm^2, respectively. In Figure 1a, first, with increasing PI concentration, the cure depths of the printed structures increased. For all cases, the cure depth tended to increase from 0.3 to 0.5 wt % of PI concentration, reached a maximum value at 0.5 wt %, and then decreased with increasing PI concentrations from 0.5 to 3 wt % (Figure 1a). At a PI concentration of 0.5 wt %, the maximum cure depths measured were 0.943, 1.529, and 2.256 mm for exposure densities of 15, 30, and 60 mJ/cm^2, respectively. When the PI concentration exceeded 0.5 wt %, the cure depth decreased rapidly with increasing PI concentration. We observed that there was an optimal PI concentration that maximized the cure depth for a given exposure energy. In this study, bottom-up DLP printing was used to print 3D structures.

The order of the printed layers was from the bottom to the top. For low-range concentrations of PI, increasing the concentration of PI resulted in a greater absorption of light on the surface of the resin. Moreover, this increase produces more radicals that initiate polymerization and light penetrates deeper into the resin, resulting in an initial increase in the cure depth. At low PI concentrations, the penetration depth can reach the point at which the degree of cross-linking and polymerization is sufficient to produce a solid network. In addition, the curing depth reaches its maximum value at a critical PI concentration. When the PI concentration exceeded the critical value, the photon penetration depth decreased. This trend occurred because of the saturable absorption of photons by the composite. At higher PI concentrations, a greater number of radicals were initiated for the rapid polymerization of the bottom layers; however, this saturated the surface of the suspension (Figure 1b). Saturable absorption occurred because the energy states near the edge were filled due to the high concentration of photogenerated carriers. Upon initiation of polymerization, the formation of the cured resin scatters and blocks further light through the resin. The absorption is blocked, and photons are transmitted through the materials without absorption (Figure 1b). The first layer received more absorption than the other layers; hence, UV radiation cannot sufficiently penetrate deeper into the top layers to perform polymerization. Photon propagation through the resin at high exposure prevents UV radiation from reaching the top layers of the printed structures and limits the increase in the curing depth.

https://doi.org/10.1021/acsomega.3c05378
ACS Omega 2024, 9, 3287−3294

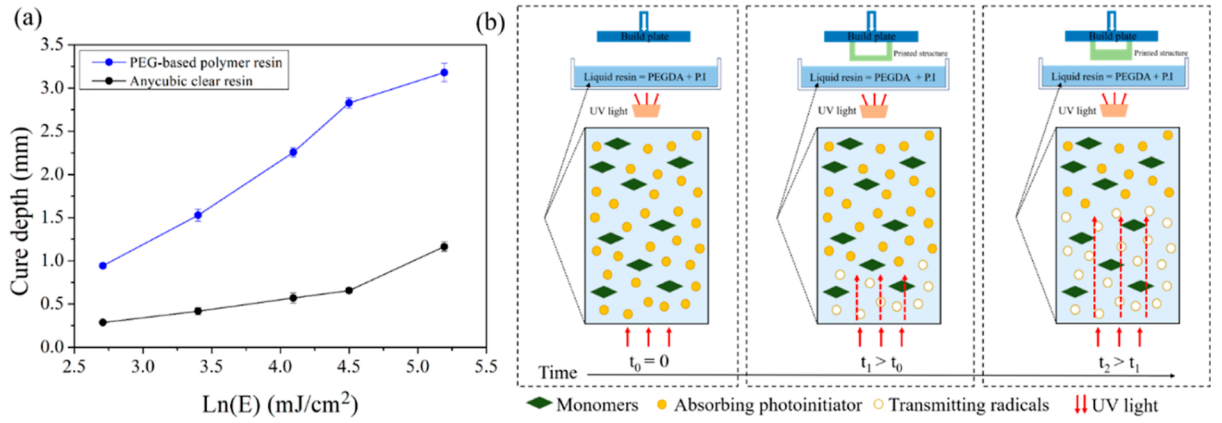

Figure 2. (a) Working curves for pure PEGDA with 0.5 wt % of PI concentration and Anycubic clear resin. (b) Schematic representation of the photopolymerization process.

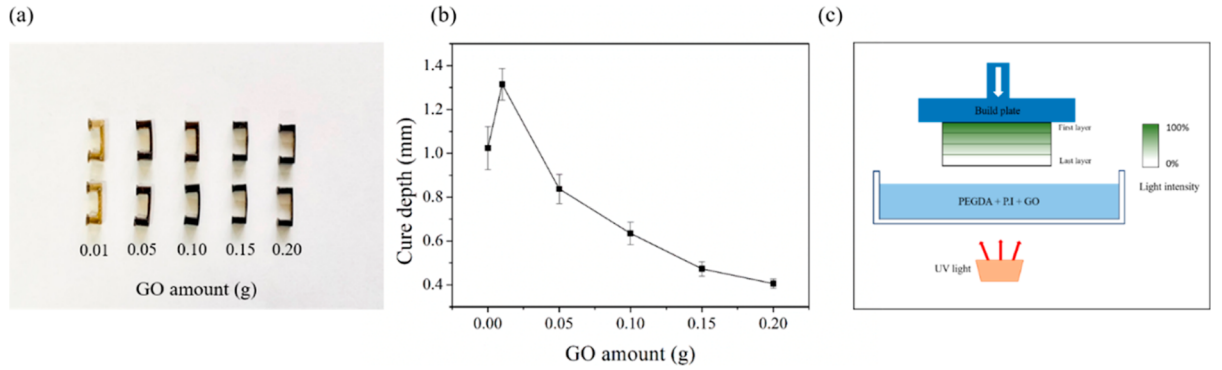

Figure 3. (a,b) Effect of different GO amounts on the cure depth of the printed structures and (c) schematic of UV curing during the 3D printing process with the composite including PEGDA, PI, and GO.

It should be noted that the maximum degree of photopolymerization corresponded to the critical PI concentration. At a high PI concentration, the saturable absorption of photons caused a nonuniform distribution of radicals within the reaction polymer mixture. This nonuniformity results in an overall lower rate of reaction in photopolymerization. Excess free radicals generated by high PI concentrations cause an increase in the coupling probability of the primary radicals, and the probability of chain termination also increases. A high concentration of PI increases the probability of free-radical collisions, which causes them to self-annihilate rather than contribute to the polymerization process. Because the curing time was identical for each PI concentration, the extent of the reaction was expected to decrease with an increasing PI concentration. Moreover, during the polymerization reaction, the cross-linked resin scatters or prevents further light penetration through the liquid resin, resulting in a decrease in the intensity ratios absorbed by the resin with an increasing degree of curing. Thus, the cure depth decreases at higher PI concentrations after a maximum is achieved at the critical point.

3.2. Cure Depth vs Exposure Condition. The working curve provides information about the extent to which exposure energy is required to cure a certain layer, the critical exposure energy for resin solidification, and the penetration depth of the printed structures. Figure 2a illustrates the effect of the exposure conditions on the curing depth of the printed structures fabricated by mixing pure PEGDA with a PI concentration of 0.5 wt %. Exposure time is a parameter used to adjust the light exposure energy, whereas the intensity of the light source of the 3D printer is fixed.

The exposure time determines the duration of light exposure in a single layer. The depth depends on the amount of energy exposure. The curing depth was determined by solidifying the liquid resin at different exposure times and measuring the thickness of the printed structures. In this study, we examined changes in the exposure times of 5, 10, 20, 30, and 60 s, and the intensity of the light source was 3 mW/cm^2.

The curing depth of the printed structures increased from 0.764 to 2.475 mm as the exposure energy increased from 15 to 180 mJ/cm^2 for PEG-based polymer resin. As predicted, the cure-depth behavior agreed with the theoretical logarithmic equations. According to Beer−Lambert's law, the absorption of a material is directly proportional to its thickness and the concentration of the attenuating species. The extended exposure time causes deeper light penetration through the polymeric liquid resin, resulting in a thicker cured part. Moreover, the number of radicals formed at a certain depth was determined by the absorbed light energy. A higher exposure energy creates more free radicals that absorb photons in charge of the polymerization reaction, leading to a higher degree of monomer-to-polymer conversion (Figure 2b). Thus, photopolymerization occurs during the 3D printing process to characterize highly cross-linked photopolymers with rapid curing behavior, thereby increasing the cure depth.

The cure-depth measurement of Anycubic clear resin, a typical 3D printing photopolymer resin, was also examined. When the exposure energy increased from 15 to 180 mJ/cm^2,

https://doi.org/10.1021/acsomega.3c05378
ACS Omega 2024, 9, 3287−3294

the curing depth of the printed structures increased from 0.286 to 1.164 mm, respectively (Figure 2a). As a result, for both cases of PEG-based polymer resin and clear resin, the cure depth increases as exposure energy increases following a logarithm of Beer−Lambert's law. In addition, at the same exposure energy, the cure depth of the 3D printed structures when printing with PEG-based polymer resin is significantly thicker than that of Anycubic clear resin.

3.3. Cure Depth vs GO Amount. The introduction of GO into the polymeric acrylic resin caused a color change in the printed structures; the more GO in the liquid resin, the darker the printed structures (Figure 3a). The liquid resins were prepared by mixing PEGDA and 1 wt % PI concentration with different quantities of GO from 0.01 to 0.2 g under the printing exposure time of 10 s. The addition of GO to the composite increased the viscosity of the suspension. The composite must be sufficiently transparent to UV radiation, and light penetration must lead to a sufficient cure depth. The UV light penetration changed with different GO concentrations in the formulation.

Figure 3b illustrates the dependence of the curing depth on the amount of GO. A slight increase in the cure depth of pure PEGDA was observed compared to the introduction of 0.01 g of GO. By increasing the amount of GO from 0.01 to 0.2 g, the measured cure depths were reduced from 1.315 to 0.406 mm. This decrease in cure depth might have been caused by the scattering and absorption of light, owing to the introduction of GO into the polymeric matrix.

The decreasing cure depth during photopolymerization is limited by the attenuation of light according to the Beer−Lambert law (Figure 3c). The absorbance and consequent attenuation of incident light by the photopolymer material are essential for free-radical photopolymerization. For UV transparency, the depth of cure is largely determined by the scattering of UV radiation. UV curing systems consisting of particles caused rapid attenuation of the incident light, which was more turbid in the composite containing GO, and light can be scattered by particles and exhibit a decrease in light penetration. Scattering, which depends primarily on the difference in refractive index between the powder and liquid resin, plays an important role in adjusting the cure depth of printed structures. The large difference in the refractive indices of GO (refractive index, n = 1.96) and PEGDA (n = 1.47) resulted in a large scattering of the incident photons. As a result, the penetration depth of light is reduced owing to scattering. Thus, less UV light penetrates the resin mixture, permitting less energy to be absorbed by the uncured resin during photopolymerization. Light intensity decreased from the bottom to the top layers. The rate of light absorption is proportional to the photon flux at a given wavelength. When comparing the two mixtures with low and high concentrations of GO, the total absorption in the case with a higher GO concentration is smaller than that in the case with a lower GO concentration, and the fraction absorption by the PI decreases owing to scattering. As the UV light passes through the material, the photon flux is diminished by absorption. In addition, the selective absorption of light by a particular material occurs when the frequency of the light source matches the specific frequency at which the electrons in the atoms of that material vibrate. The DLP 3D printer used in this study had a light source with a wavelength of 405 nm. Table 1 shows that the absorption spectrum of GO is 230 nm and that of PI is 430 nm; therefore, GO is an unreactive chemical that is highly absorbed in the laser wavelength of the printer. Successful 3D printing requires the absorption of the liquid resin to match the emission spectrum of the 3D printing source. With long-wavelength PI, these molecules absorb UV radiation instead of GO because GO cannot absorb at these wavelengths. The depth of cure for suspensions containing GO powder is limited by scattering. Therefore, with increasing GO concentration, the UV light that penetrated the liquid resin mixture was reduced, allowing less energy to be absorbed by the uncured resin.

Table 1. Physical Properties of PEGDA and GO, Irgacure 819 PI[34−39]

	PEGDA	GO	PI	PEGDA + PI
refractive index	1.47	1.96	1.588	-
absorption peak (nm)	213	230	430	412

Figure 4a shows the working curve of the cure depth vs the logarithm of the exposure energy. The curing depth of the printed structures decreased with increasing GO content and increased with increasing exposure energy. An increased absorbed photon dose cures more liquid resin, thereby increasing the measured cure depth. In the case of a 5 s exposure time, the GO amount of 0.2 g could not be printed successfully for the samples because the cure depth of the printed structures decreased to a small thickness at which the structures could not be formed. Therefore, a higher concentration of GO reduces the cure depth to a greater extent than the desired amount, resulting in undesirable microstructures. In addition, in the case of 60 s exposure time of 0.01 g GO, there was an amount of generated radicals; therefore, the surrounding area was affected by curing, resulting in unsuccessful printed structures for cure-depth measurement. Figure 4b,c shows the calculated critical energy and penetration depth, respectively, for the five resins with different GO concentrations. It is illustrated that when the amount of GO increased from 0.01 to 0.2 g, the critical energy and the depth of penetration decreased. At a high concentration of GO in the polymeric resin, light can be scattered. Thus, the absorption coefficient of photons decreased compared with lower concentrations of GO. These results agree with the theoretical predictions that the critical exposure energy, E_c, generates sufficient free radicals to initiate a chemical reaction. Decreasing the amount of GO in the composite allowed light to penetrate deeper into the uncured resin, thereby increasing the level of light penetration.

3.4. Discussion. For the particular PI/monomer system, the relationship between the cure depth and the penetration depth has been derived as follows[40]

$$C_d \propto \frac{d}{Q}\frac{1}{\phi}\ln\left(\frac{E_0}{E_c}\right) \tag{2}$$

where d is the mean ceramic suspension particle size, Q is the scattering efficiency term, and Φ is the volume fraction of the ceramic powder.

Deriving from eqs 1 and 2, the relationship between the penetration depth and volume fraction depth can be expressed as follows

$$D_p \propto \frac{d}{Q}\frac{1}{\phi} \tag{3}$$

https://doi.org/10.1021/acsomega.3c05378
ACS Omega 2024, 9, 3287−3294

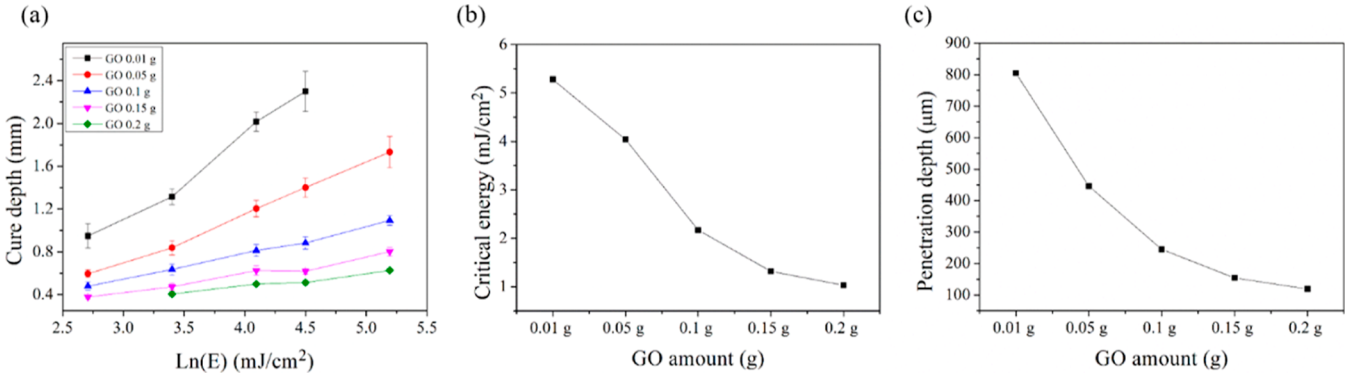

Figure 4. (a) Graph of cure depth versus the logarithm of exposure energy and (b) critical energy and (c) penetration depth for different GO amounts.

Thus, the penetration depth of the printed structures is inversely proportional to the volume fraction of the solid. The linear relationship between the cure depth and the inverse volume fraction is well-established for a highly concentrated suspension system.

Figure 5 shows the calculated penetration depths as a function of the inverse volume fraction of GO, 1/Φ. The depth

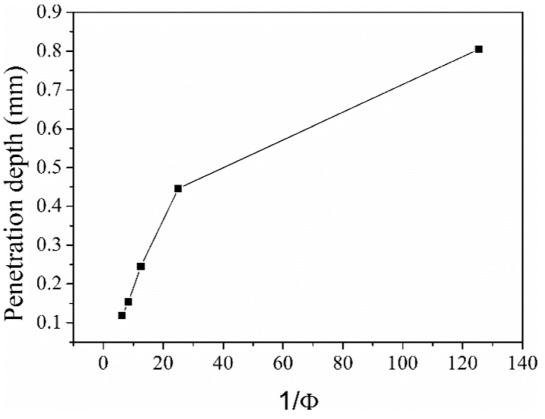

Figure 5. Calculated penetration depth as a function of the inverse volume fraction of GO.

of penetration of the printed structures is directly proportional to the inverse volume fraction of GO, but the graph shows two different slopes. The slope in the large volume range of 0.05−0.2 g of GO is steep, at approximately 0.017, while the slope in the small volume range of 0.01−0.05 g of GO is shallower, at approximately 0.004. This result indicates that the scattering efficiency varied discontinuously, because the mean suspension particle size was constant. When producing complex 3D printed structures with a mixed resin system containing a low concentration of colloidal suspension, it may be necessary to precisely clarify the effect of scattering efficiency.

The reduction in penetration depth by adding GO affects the quality and resolution of the printed structures. The introduction of GO into the 3D printing process emerges as a transformative factor, significantly enhancing the quality of printed structures. The scaffolds were fabricated using two printing resin types, namely, pure PEGDA and a composite of PEGDA and 0.2 g GO. The combination of PEGDA and GO improves the precision and introduces more detail and accuracy in printed structures compared to using pure PEGDA (Figure 6). This highlights the crucial role of GO in elevating the quality resolution of printed structures, establishing it as a critical element for 3D printing results.

4. CONCLUSIONS

The cure-depth characteristics of photopolymer resins based on PEGDA and GO were investigated by using the DLP 3D printing method. This study contributes to the understanding and investigation of the printed quality of structures fabricated via photopolymerization. In the examination of the cure depth of the printed structures, several parameters were found to influence the curing behavior, such as the light intensity, concentration of PI, and composition of the photopolymer resin. The effect of varying the exposure conditions on the cure depth was investigated, and it was found that the cure depth increased as the exposure energy increased, as expected from the logarithmic equation. The results showed that there was a critical PI concentration at which the cure depth reached a maximum and then decreased with an increasing PI

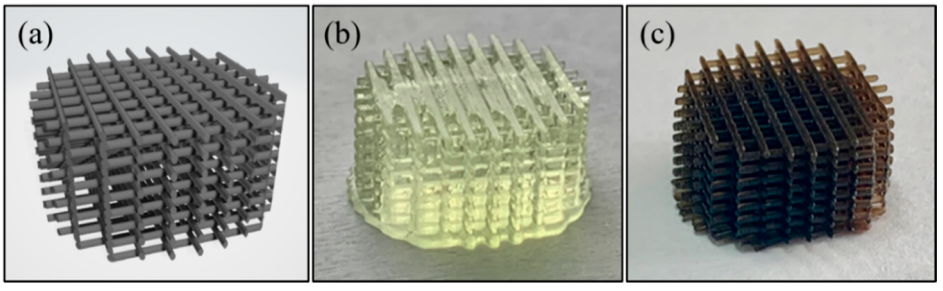

Figure 6. Print quality of different printing resins: (a) digital modeling, (b) 3D printing of pure PEGDA, and (c) 3D printing of the composite including PEGDA and GO.

https://doi.org/10.1021/acsomega.3c05378
ACS Omega 2024, 9, 3287−3294

concentration. When the PI concentration exceeded 0.5 wt %, the cure depth decreased rapidly with increasing PI concentration. Saturable absorption of photons occurs in the photosensitive resin, leading to a maximum cure depth. The effect of GO on the polymeric composite was investigated by controlling the curing depth of the printed structure. With an increase in the amount of GO introduced into the photopolymer mixture, the curing depth decreased owing to the scattering and attenuation of the exposed light energy in the liquid resin. The addition of GO reduced the critical energy and penetration depth of the UV-cured resins. The introduction of GO limited light penetration into the photopolymer formulation, thus improving the thickness of the cured samples. The study of the cure-depth behavior in photopolymerization is an important aspect of the curing process, and the experimental approach can be applied to the fabrication of printed structures to improve the resolution of cured samples for curable coatings and industrial applications.

AUTHOR INFORMATION

Corresponding Authors

Sang Jung Ahn − *Korea Research Institute of Standard and Science (KRISS), Daejeon 34113, Republic of Korea*; Email: sjahn@kriss.re.kr

Young Heon Kim − *Graduate School of Analytical Science and Technology (GRAST), Chungnam National University, Daejeon 34134, Republic of Korea*; orcid.org/0000-0001-9944-5859; Email: y.h.kim@cnu.ac.kr

Authors

Men Thi Hong Nguyen − *Graduate School of Analytical Science and Technology (GRAST), Chungnam National University, Daejeon 34134, Republic of Korea*

Jong Hoon Kim − *Graduate School of Analytical Science and Technology (GRAST), Chungnam National University, Daejeon 34134, Republic of Korea*

Woo Tae Jang − *Graduate School of Analytical Science and Technology (GRAST), Chungnam National University, Daejeon 34134, Republic of Korea*

Yun Jae Jung − *Graduate School of Analytical Science and Technology (GRAST), Chungnam National University, Daejeon 34134, Republic of Korea*

Eun Jin Park − *Core Research Facility Management Center, Korea Research Institute of Bioscience and Biotechnology (KRIBB), Daejeon 34141, Republic of Korea; Department of Nanobiotechnology, KRIBB School of Biotechnology, Korea University of Science and Technology (UST), Daejeon 34113, Republic of Korea*

Tai Hwan Ha − *Core Research Facility Management Center, Korea Research Institute of Bioscience and Biotechnology (KRIBB), Daejeon 34141, Republic of Korea; Department of Nanobiotechnology, KRIBB School of Biotechnology, Korea University of Science and Technology (UST), Daejeon 34113, Republic of Korea*; orcid.org/0000-0003-0892-3320

Complete contact information is available at: https://pubs.acs.org/10.1021/acsomega.3c05378

Notes

The authors declare no competing financial interest.

ACKNOWLEDGMENTS

This work was supported by the research fund of Chungnam National University.

ABBREVIATIONS

3D, 3-dimensional; DLP, digital light processing; PEGDA, polyethylene glycol diacrylate; GO, graphene oxide; PI, photoinitiator; UV, ultraviolet

REFERENCES

(1) Lang, M.; Hirner, S.; Wiesbrock, F.; Fuchs, P. A Review on Modeling Cure Kinetics and Mechanisms of Photopolymerization. *Polymers* **2022**, *14* (10), 2074−2158.

(2) Clapper, J. D.; Sievens-Figueroa, L.; Guymon, C. A. Photopolymerization in Polymer Templating. *Chem. Mater.* **2008**, *20* (3), 768−781.

(3) Kenning, N. S.; Kriks, D.; El-Maazawi, M.; Scranton, A. Spatial and Temporal Evolution of the Photoinitiation Rate for Thick Polymer Systems Illuminated with Polychromatic Light. *Polym. Int.* **2006**, *55* (9), 994−1006.

(4) Seol, S. K.; Kim, D.; Lee, S.; Kim, J. H.; Chang, W. S.; Kim, J. T. Electrodeposition-Based 3D Printing of Metallic Microarchitectures with Controlled Internal Structures. *Small* **2015**, *11* (32), 3896−3902.

(5) Brady, G. A.; Chu, T. M.; Halloran, J. W. Curing Behavior of Ceramic Resin for Stereolithography. *1996 International Solid Freeform Fabrication Symposium*; University of Texas, 1996; pp 403−410.

(6) Wudy, K.; Budde, T. Reaction Kinetics and Curing Behavior of Epoxies for Use in a Combined Selective Laser Beam Melting Process of Polymers. *J. Appl. Polym. Sci.* **2019**, *136* (7), 1−10.

(7) Choi, J. W.; Wicker, R. B.; Cho, S. H.; Ha, C. S.; Lee, S. H. Cure Depth Control for Complex 3D Microstructure Fabrication in Dynamic Mask Projection Microstereolithography. *Rapid Prototyp. J.* **2009**, *15* (1), 59−70.

(8) Luongo, A.; Falster, V.; Doest, M. B.; Ribo, M. M.; Eiriksson, E. R.; Pedersen, D. B.; Frisvad, J. R. Microstructure Control in 3D Printing with Digital Light Processing. *Comput. Graph. Forum* **2020**, *39* (1), 347−359.

(9) Kowsari, K.; Akbari, S.; Wang, D.; Fang, N. X.; Ge, Q. High-Efficiency High-Resolution Multimaterial Fabrication for Digital Light Processing-Based Three-Dimensional Printing. *3D Print. Addit. Manuf.* **2018**, *5* (3), 185−193.

(10) Wang, Y.; Li, X.; Chen, Y.; Zhang, C. Strain Rate Dependent Mechanical Properties of 3D Printed Polymer Materials Using the DLP Technique. *Addit. Manuf.* **2021**, *47*, 102368.

(11) Mu, Q.; Wang, L.; Dunn, C. K.; Kuang, X.; Duan, F.; Zhang, Z.; Qi, H. J.; Wang, T. Digital Light Processing 3D Printing of Conductive Complex Structures. *Addit. Manuf.* **2017**, *18*, 74−83.

(12) Zhang, J.; Hu, Q.; Wang, S.; Tao, J.; Gou, M. Digital Light Processing Based Three-Dimensional Printing for Medical Applications. *Int. J. Bioprint.* **1970**, *6* (1), 242−327.

(13) Yoo, S. Y.; Kim, S. K.; Heo, S. J.; Koak, J. Y.; Kim, J. G. Dimensional Accuracy of Dental Models for Three-Unit Prostheses Fabricated by Various 3D Printing Technologies. *Mater.* **2021**, *14* (6), 1550−1613.

(14) Bazaz, S. R.; Kashaninejad, N.; Azadi, S.; Patel, K.; Asadnia, M.; Jin, D.; Warkiani, M. E. Rapid Softlithography Using 3D-Printed Molds. *Adv. Mater. Technol.* **2019**, *4* (10), 1−11.

(15) Choong, Y. Y. C.; Maleksaeedi, S.; Eng, H.; Su, P. C.; Wei, J. Curing Characteristics of Shape Memory Polymers in 3D Projection and Laser Stereolithography. *Virtual Phys. Prototyp.* **2017**, *12* (1), 77−84.

(16) Bennett, J. Measuring UV Curing Parameters of Commercial Photopolymers Used in Additive Manufacturing. *Addit. Manuf.* **2017**, *18*, 203−212.

https://doi.org/10.1021/acsomega.3c05378
ACS Omega 2024, 9, 3287−3294

(17) Chartier, T.; Chaput, C.; Doreau, F.; Loiseau, M. Stereolithography of Structural Complex Ceramic Parts. *J. Mater. Sci.* **2002**, *37* (15), 3141−3147.
(18) Han, D.; Yang, C.; Fang, N. X.; Lee, H. Rapid Multi-Material 3D Printing with Projection Micro-Stereolithography Using Dynamic Fluidic Control. *Addit. Manuf.* **2019**, *27*, 606−615.
(19) Guthrie, J.; Jeganathan, M. B.; Otterburn, M. S.; Woods, J. Light Screening Effects of Photoinitiators in UV Curable Systems. *Polym. Bull.* **1986**, *15* (1), 51−58.
(20) Sim, J.-H.; Lee, E.-D.; Kweon, H.-J. Effect of the Laser Beam Size on the Cure Properties of a Photopolymer in Stereolithography. *Int. J. Precis. Eng. Manuf.* **2007**, *8*, 50−55.
(21) Bagheri, A.; Jin, J. Photopolymerization in 3D Printing. *ACS Appl. Polym. Mater.* **2019**, *1* (4), 593−611.
(22) Ammar, A.; Al-Enizi, A. M.; AlMaadeed, M. A. A.; Karim, A. Influence of Graphene Oxide on Mechanical, Morphological, Barrier, and Electrical Properties of Polymer Membranes. *Arab. J. Chem.* **2016**, *9* (2), 274−286.
(23) Maheshkumar, K. V.; Krishnamurthy, K.; Sathishkumar, P.; Sahoo, S.; Uddin, E.; Pal, S. K.; Rajasekar, R. Research Updates on Graphene Oxide-Based Polymeric Nanocomposites. *Polym. Compos.* **2014**, *35* (12), 2297−2310.
(24) Allahbakhsh, A.; Sharif, F.; Mazinani, S. The Influence of Oxygen-Containing Functional Groups on the Surface Behavior and Roughness Characteristics of Graphene Oxide. *Nano* **2013**, *08* (04), 1350045−1350048.
(25) Hwang, J.; Yoon, T.; Jin, S. H.; Lee, J.; Kim, T. S.; Hong, S. H.; Jeon, S. Enhanced Mechanical Properties of Graphene/Copper Nanocomposites Using a Molecular-Level Mixing Process. *Adv. Mater.* **2013**, *25* (46), 6724−6729.
(26) Konios, D.; Stylianakis, M. M.; Stratakis, E.; Kymakis, E. Dispersion Behaviour of Graphene Oxide and Reduced Graphene Oxide. *J. Colloid Interface Sci.* **2014**, *430*, 108−112.
(27) Komissarenko, D. A.; Sokolov, P. S.; Evstigneeva, A. D.; Shmeleva, I. A.; Dosovitsky, A. E. Rheological and Curing Behavior of Acrylate-Based Suspensions for the DLP 3D Printing of Complex Zirconia Parts. *Mater.* **2018**, *11* (12), 2350.
(28) Li, K.; Zhao, Z. The Effect of the Surfactants on the Formulation of UV-Curable SLA Alumina Suspension. *Ceram. Int.* **2017**, *43* (6), 4761−4767.
(29) Wu, L.; Liu, L.; Gao, B.; Muñoz-Carpena, R.; Zhang, M.; Chen, H.; Zhou, Z.; Wang, H. Aggregation Kinetics of Graphene Oxides in Aqueous Solutions: Experiments, Mechanisms, and Modeling. *Langmuir* **2013**, *29* (49), 15174−15181.
(30) Maio, A.; Fucarino, R.; Khatibi, R.; Rosselli, S.; Bruno, M.; Scaffaro, R. A Novel Approach to Prevent Graphene Oxide Re-Aggregation during the Melt Compounding with Polymers. *Compos. Sci. Technol.* **2015**, *119*, 131−137.
(31) Ribas-Massonis, A.; Cicujano, M.; Duran, J.; Besalú, E.; Poater, A. Free-Radical Photopolymerization for Curing Products for Refinish Coatings Market. *Polymers* **2022**, *14* (14), 2856.
(32) Eibel, A.; Fast, D. E.; Gescheidt, G. Choosing the Ideal Photoinitiator for Free Radical Photopolymerizations: Predictions Based on Simulations Using Established Data. *Polym. Chem.* **2018**, *9* (41), 5107−5115.
(33) Diegel, O.; Nordin, A.; Motte, D. Additive Manufacturing Technologies. *Additive Manufacturing Technologies*; Springer, 2019; pp 19−39.
(34) Takahashi, H.; Kan, T.; Lee, G.; Dönmez, N.; Kim, J.; Park, J.; Kim, D.; Heo, Y. J. Self-Focusing 3D Lithography with Varying Refractive Index Polyethylene Glycol Diacrylate. *Appl. Phys. Express* **2020**, *13* (7), 076503.
(35) Pelras, T.; Glass, S.; Scherzer, T.; Elsner, C.; Schulze, A.; Abel, B. Transparent Low Molecularweight Poly(Ethylene Glycol) Diacrylate-Based Hydrogels as Film Media for Photoswitchable Drugs. *Polymers* **2017**, *9* (12), 639.
(36) Schmiedova, V.; Pospisil, J.; Kovalenko, A.; Ashcheulov, P.; Fekete, L.; Cubon, T.; Kotrusz, P.; Zmeskal, O.; Weiter, M. Physical Properties Investigation of Reduced Graphene Oxide Thin Films Prepared by Material Inkjet Printing. *J. Nanomater.* **2017**, *2017*, 1−8.
(37) Zhang, T.; Zhu, G. Y.; Yu, C. H.; Xie, Y.; Xia, M. Y.; Lu, B. Y.; Fei, X.; Peng, Q. The UV Absorption of Graphene Oxide Is Size-Dependent: Possible Calibration Pitfalls. *Microchim. Acta* **2019**, *186* (3), 207.
(38) CIBA Specialty Chemicals. *Photoinitiators for UV Curing*; CIBA, 2003; pp 1−8.
(39) Gong, H.; Beauchamp, M.; Perry, S.; Woolley, A. T.; Nordin, G. P. Optical Approach to Resin Formulation for 3D Printed Microfluidics. *RSC Adv.* **2015**, *5* (129), 106621−106632.
(40) Griffith, M. L.; Halloran, J. W. Freeform Fabrication of Ceramics via Stereolithography. *J. Am. Ceram. Soc.* **1996**, *79*, 2601−2608.

https://doi.org/10.1021/acsomega.3c05378
ACS Omega 2024, 9, 3287−3294